

## Y-branched TiO<sub>2</sub> nanotube arrays synthesized by anodic oxidation

YANG Xu<sup>1,2</sup>, QU Yi<sup>1</sup>, FAN Yi<sup>2\*</sup> & LIU XingYuan<sup>2</sup>

<sup>1</sup> National Key Lab of High Power Semiconductor Lasers, Changchun University of Science and Technology, Changchun 130022, China;

<sup>2</sup> Key Laboratory of Excited State Processes, Changchun Institute of Optics, Fine Mechanics and Physics, Chinese Academy of Sciences, Changchun 130033, China

Received August 19, 2011; accepted October 19, 2011; published online December 15, 2011

We report a novel synthesis strategy for Y-branched TiO<sub>2</sub> nanotubes on a pure titanium foil by electrochemical anodic oxidation in an NH<sub>4</sub>F organic electrolyte. Effects of temperature range, oxidation time, and morphology-dependent parameters of the Y-branched TiO<sub>2</sub> nanotube arrays were investigated. We found that an optimized growth-temperature window between 20°C and 30°C resulted in Y-branched nanotubes with much better morphology and photoelectric performances. After annealing at 450°C for 1.5 h in air, a dominant crystal structure of these arrays was indexed to anatase.

**Y-branched TiO<sub>2</sub> nanotube, anodization, oxidation temperature, anatase**

**PACS number(s):** 78.67.Ch, 42.79.Ek, 68.55.ag, 68.47.Gh

**Citation:** Yang X, Qu Y, Fan Y, et al. Y-branched TiO<sub>2</sub> nanotube arrays synthesized by anodic oxidation. *Sci China-Phys Mech Astron*, 2012, 55: 14–18, doi: 10.1007/s11433-011-4580-x

Much research in the past decade has focused on TiO<sub>2</sub> nanotube arrays because of their superior semiconducting material properties and potential applications involving dye-sensitized solar cells, sensors, and hydrogen storage, as well as electrocatalytic, photocatalytic, and photoelectrolytic reactions [1–3]. The TiO<sub>2</sub> nanotube arrays exhibit promising photovoltaic, photoelectrochemical, and photocatalytic properties; its ordered and strongly interconnected nanoscale architecture can further improve charge separation and charge transport, leading to a higher photovoltaic conversion efficiency, and can restrain the recombination of photogenerated electron-hole pairs [4].

After the discovery of single-axis TiO<sub>2</sub> nanotubes, Mohapatra and coworkers [5] in 2008 successfully presented the formation of Y-branched TiO<sub>2</sub> nanotubes on a pure titanium foil by electrochemical anodic oxidation. The Y-branched TiO<sub>2</sub> nanotube arrays are expected to have different electronic and photon absorption properties compared

with single-axis nanotube structures owing to the denser growth of the branched nanotubes. However, the relationship between synthesis conditions and the formation process of the Y-branched TiO<sub>2</sub> nanotubes have not been well-understood: hence the study of the essential factors that affect formation and determine its micro-mechanism is needed.

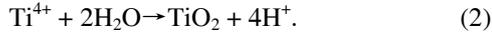
In this paper, we discuss the growth mechanism of Y-branched TiO<sub>2</sub> nanotubes, showing field emission scanning electron microscopy (FE-SEM) micrographs of Y-branched TiO<sub>2</sub> nanotube arrays obtained by a two-step electrochemical anodization method. Junctions were produced by changing the anodization temperature. We found that more Y-branched TiO<sub>2</sub> nanotubes with better morphology and photoelectric performance could be developed if grown in a suitable temperature range.

### 1 Mechanism discussion

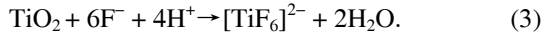
As shown in Figure 1, at an early stage of anodization, a dense high-resistant oxide film (barrier layer) was formed

\*Corresponding author (email: fan\_yi1986@sina.com)

on the titanium substrate. This initial stage involved the following two reactions: namely fast dissolution of titanium and formation of an oxide layer [6],



In the electrolyte containing  $\text{F}^{-}$  ions, the oxide layer dissolves partly and nanotubes are created from small pits that are formed in the oxide layer. These pits are continued with the direct complexation of  $\text{Ti}^{4+}$  ions migrating through the film and formed under the following reaction [7]:



As mentioned above, the dissolution of  $\text{TiO}_2$  is accompanied by its formation during the anodization. The dissolution rate  $\nu_d$  and the formation rate  $\nu_f$  of  $\text{TiO}_2$  mainly depend on the electric field strength in the electrolyte/ $\text{TiO}_2$  and  $\text{TiO}_2/\text{Ti}$  foil interfaces, respectively. For  $\nu_d > \nu_f$  (resp.  $\nu_d < \nu_f$ ), the thickness of the oxide layer will be reduced (resp. increased). Finally,  $\nu_d$  and  $\nu_f$  will gradually equilibrate and the thickness of the oxide layer approaches a stable value. The anodization continues and the nanotubes inside the Ti foil grow parallel and straight in a fixed electrolyte aqueous solution at a constant voltage and temperature [8–10].

If the anodizing temperature increases suddenly in the second step of the two-step anodization process, the equilibrium between the dissolution and the formation of the  $\text{TiO}_2$  barrier layer will break. During the temperature-elevating process of electrolysis, molecular motions are accelerated, so the  $\text{F}^{-}$  ions become active in increasing the dissolution rate  $\nu_d$  of  $\text{TiO}_2$  layer [11]. However, the anodizing voltage is always constant at 20 V, the formation rate  $\nu_f$

of  $\text{TiO}_2$  layer is stable, so  $\nu_d > \nu_f$ . At this point, the dissolution reaction dominates in the process and tends to reduce the thickness of the barrier layer. Thus, cavities will form at the bottom of the nanotubes. This process is also similar to the early formation stage of core holes from single-axis  $\text{TiO}_2$  nanotubes. For single-axis  $\text{TiO}_2$  nanotubes, after the formation of the  $\text{TiO}_2$  oxide film on the titanium substrate, the dissolution reaction dominates ( $\nu_d > \nu_f$ ) and reduces the thickness of the barrier layer. Thus core holes are formed and finally lead to the formation of nanotubes. Core holes from single-axis  $\text{TiO}_2$  nanotubes form on the overall surface of the titanium foil, but those branched  $\text{TiO}_2$  nanotubes just form at the bottom area of the single-axis nanotubes in the first step of anodization (Figure 2). If the thickness of the barrier layer is reduced to a new balanced value, the anodization continues again and the branched nanotubes grow parallel and straight with a smaller interpore distance. Evidently, this process confirms the controlled growth of branched nanotubes.

## 2 Synthesis process

In this study, anodization was conducted in a 100 mL electrolyte with  $\text{NH}_4\text{F}$  (0.5wt%), deionized water (5wt%) and ethylene glycol. The titanium foil electrode (99.7% purity, Alfa Aesar; 0.032 mm thickness; 1 cm×2 cm area) served as the anode, and the counter electrode platinum (Pt) foil (0.5 mm thickness; 1 cm×1 cm area) served as the cathode. The distance between the two electrodes was kept at 3–5 cm in all experiments (Figure 3).

Prior to anodization, the titanium foils were degreased ultrasonically in acetone and then ethanol, each for 5 min,

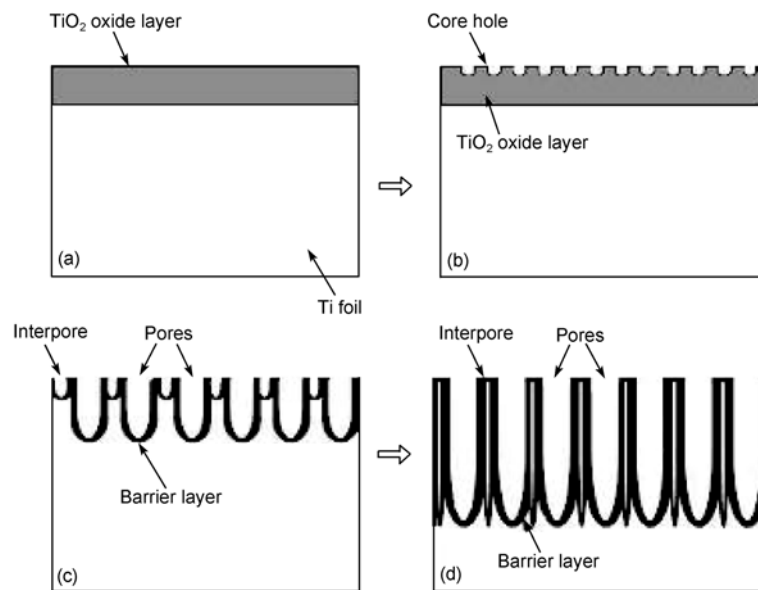


**Figure 1** Illustration of single-axis  $\text{TiO}_2$  nanotubes growth mechanism. (a)  $\text{TiO}_2$  oxide layer formation; (b) core holes formation on the oxide layer; (c) growth of the core holes into scallop-shaped pores; (d) single-axis  $\text{TiO}_2$  nanotubes formation.

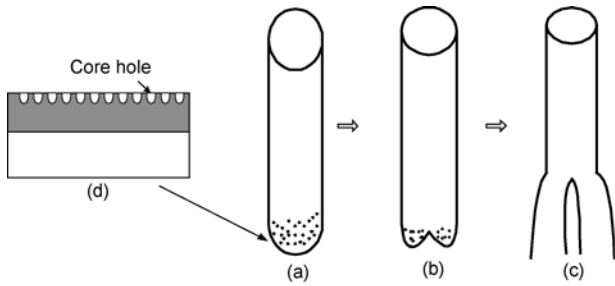


**Figure 2** Illustration of Y-branched  $\text{TiO}_2$  nanotube growth mechanism. (a) Single-axis  $\text{TiO}_2$  nanotubes formation; (b) core holes formation at the bottom of single-axis  $\text{TiO}_2$  nanotubes; (c) Y-branched  $\text{TiO}_2$  nanotubes formation; (d) the formation stage of single-axis  $\text{TiO}_2$  nanotubes' core holes.

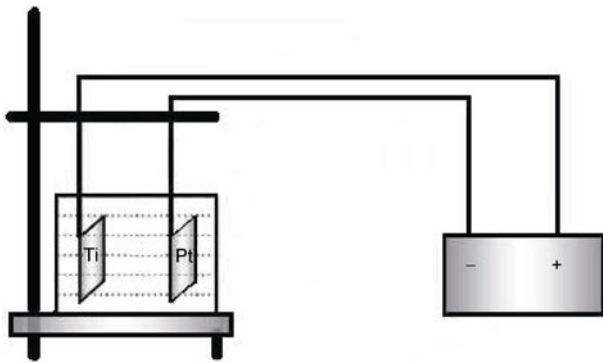


**Figure 3** Illustration of the anodic oxidation apparatus in which Ti samples were anodized.

followed by rinsing with deionized water, and then drying in an air stream. The experiments were performed at approximately  $20^\circ\text{C}$  at a constant voltage of 20 V for 30 min, before the temperature of the solution was increased from  $20^\circ\text{C}$  to  $30^\circ\text{C}$ . The anodization was further continued for another 30 min at  $30^\circ\text{C}$  and 20 V. Finally, the anodized samples were annealed in air at  $450^\circ\text{C}$  for 1.5 h in the annealing oven. The morphology and structure of the  $\text{TiO}_2$  nanotube samples were characterized using FE-SEM (Hitachi S-4800) and X-ray diffraction (XRD) analysis.

### 3 Results and discussion

FE-SEM was utilized to image the morphology of the synthesized Y-branched  $\text{TiO}_2$  nanotube arrays. The top view in Figure 2(a) looks similar to the single-axis  $\text{TiO}_2$  nanotube array [2]. Figures 4(b)–(d) show cross-sections of the Y-branched  $\text{TiO}_2$  nanotube arrays, from which the Y-branched structure can be clearly observed. The average length of these nanotubes is about  $1.4\ \mu\text{m}$ . The inner diameter of each  $\text{TiO}_2$  nanotube is in the range between 50 nm and 55 nm, respectively. The wall thickness is around 15 nm.

It has been shown that from  $25^\circ\text{C}$  to  $35^\circ\text{C}$  is a good temperature range for the preparation of the Y-branched  $\text{TiO}_2$  nanotube array [2]. However, we experimentally found

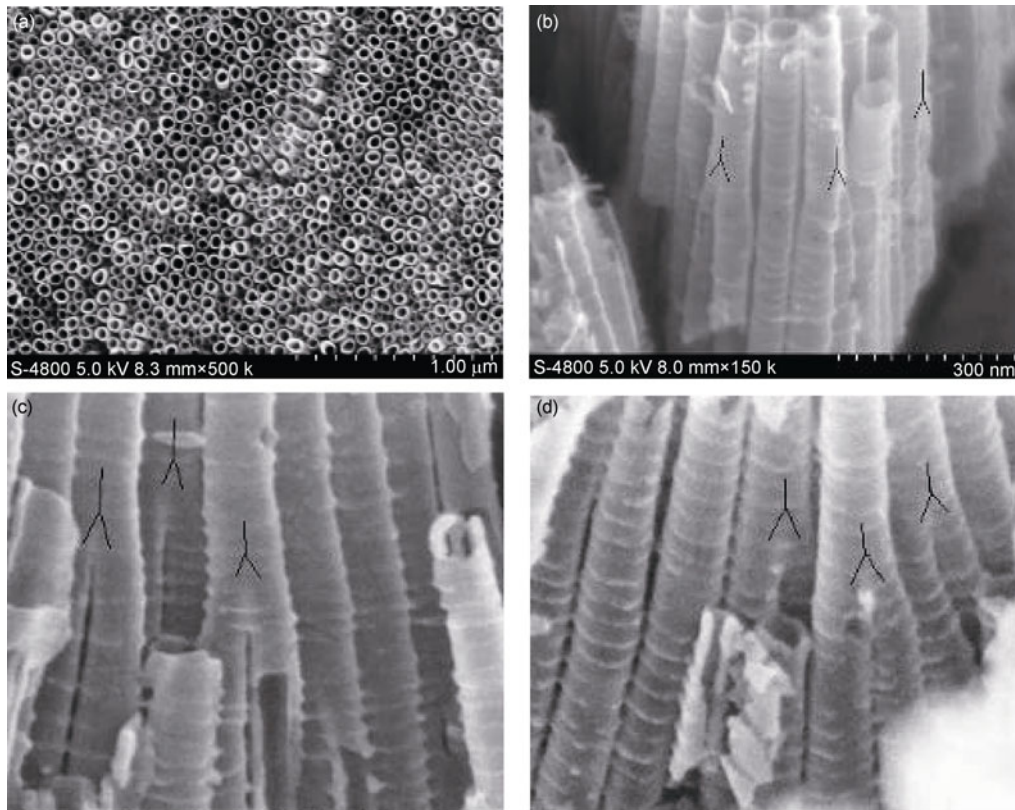


**Figure 4** SEM images of top and cross-section of the Y-branched  $\text{TiO}_2$  nanotube arrays. (a) The top-section image of Y-branched  $\text{TiO}_2$  nanotubes; (b)–(d) the cross-section images of Y-branched  $\text{TiO}_2$  nanotubes.

more uniform Y-branched  $\text{TiO}_2$  nanotubes can be observed in the temperature range from  $20^\circ\text{C}$  to  $30^\circ\text{C}$ . Moreover, a better morphology and photoelectric performance of  $\text{TiO}_2$  nanotube arrays can be expected in this temperature range, because the electrolyte temperature significantly influences the wall thickness at the top of the tube. Figure 5 shows many ruptures and defects occurring near the top if the electrolyte temperature is above  $30^\circ\text{C}$ . The thinner  $\text{TiO}_2$  nanotubes were prone to increased surface recombination rates of separated electrons and holes [12]. Therefore, the nanotubes fabricated at lower anodization temperatures would have greater wall thicknesses, resulting in larger photocurrents and better morphology [13].

The electrolyte temperature significantly influences wall thickness at the top of the tube, but has a negligible effect on tube growth. Figure 6 shows FE-SEM images of  $\text{TiO}_2$  nanotube arrays obtained by anodic oxidation of Ti foil in 0.5wt%  $\text{NH}_4\text{F}$  contained ethylene glycol solution. Figures 4(b)–(d) give the cross-sectional images obtained by anodization at a constant voltage of 20 V for 1 h, 3 h, and 5.5 h, respectively. The length of the  $\text{TiO}_2$  nanotubes increased to  $1.4\ \mu\text{m}$  for 1 h to  $3.2\ \mu\text{m}$  for 5.5 h. Longer nanotube arrays can be obtained by controlling, for example,  $\text{NH}_4\text{F}$  concentration, anodizing time, and anodizing voltage [14,15].

The effects of heat treatment on the crystal structures of  $\text{TiO}_2$  nanotubes were investigated by XRD analysis.  $\text{TiO}_2$  nanotubes were annealed at  $450^\circ\text{C}$  under ambient air for 1.5 h. The XRD graph in Figure 7 indicates that the as-prepared  $\text{TiO}_2$  nanotubes arrays are mainly in the anatase phase, as evidenced by the strong diffraction peaks at  $2\theta=25.3401^\circ$ ,  $2\theta=48.1602^\circ$ ,  $2\theta=53.8802^\circ$ , which can be indexed respectively to the (101), (200), and (105) crystal faces of anatase  $\text{TiO}_2$ . Diffraction intensities from the anatase (101) crystal face are seen to become stronger with increasing nanotube array length [16], as well as the amount of  $\text{TiO}_2$ .

## 4 Conclusions

In summary, we report a facile growth mechanism of Y-branched  $\text{TiO}_2$  nanotube arrays on a pure titanium foil prepared by electrochemical anodic oxidation in an  $\text{NH}_4\text{F}$  organic electrolyte. Our results show that a temperature range between  $20^\circ\text{C}$  and  $30^\circ\text{C}$  facilitated better growth of Y-branched  $\text{TiO}_2$  nanotubes with better morphology and photoelectric performance. Above the electrolyte temperature of  $30^\circ\text{C}$ , substantial rupturing and defect formation occurred near the tops of the tubes. After an annealing

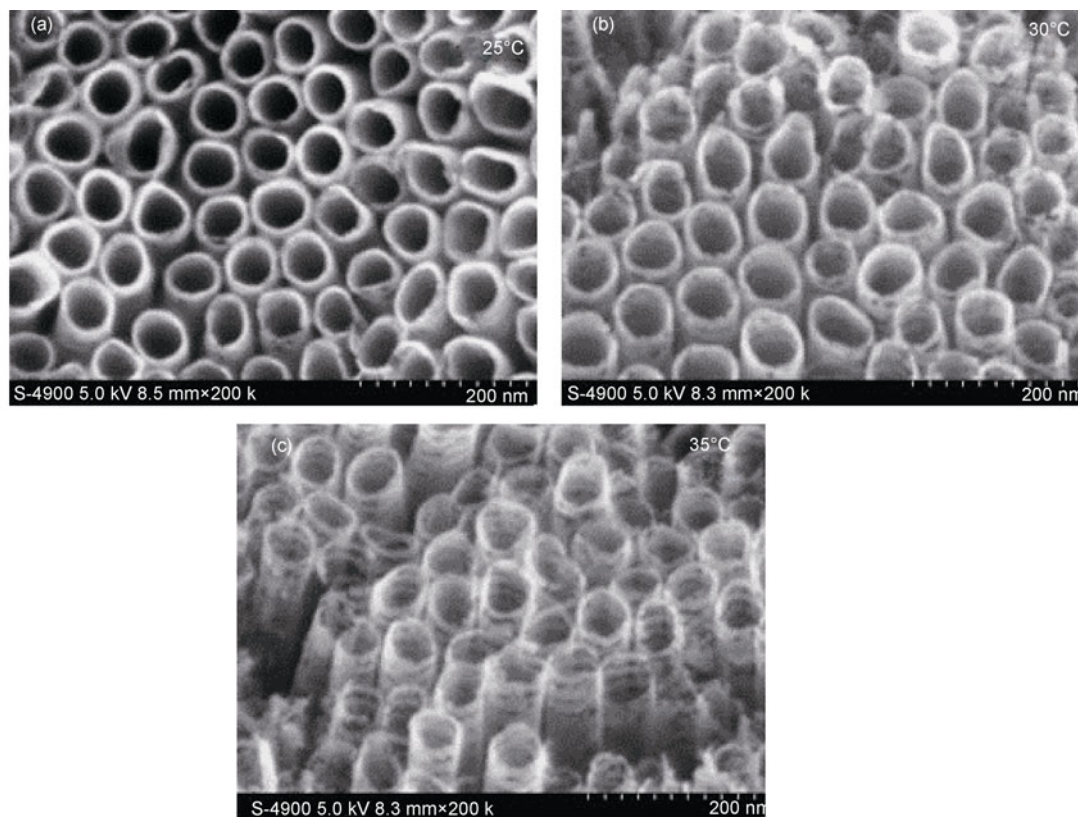


**Figure 5** Side-view FE-SEM images of  $\text{TiO}_2$  nanotube arrays obtained at  $25^\circ\text{C}$ ,  $30^\circ\text{C}$ , and  $35^\circ\text{C}$  with 20 V for 1 h in the electrolyte containing 0.5wt%  $\text{NH}_4\text{F}$  and 5wt%  $\text{H}_2\text{O}$ .

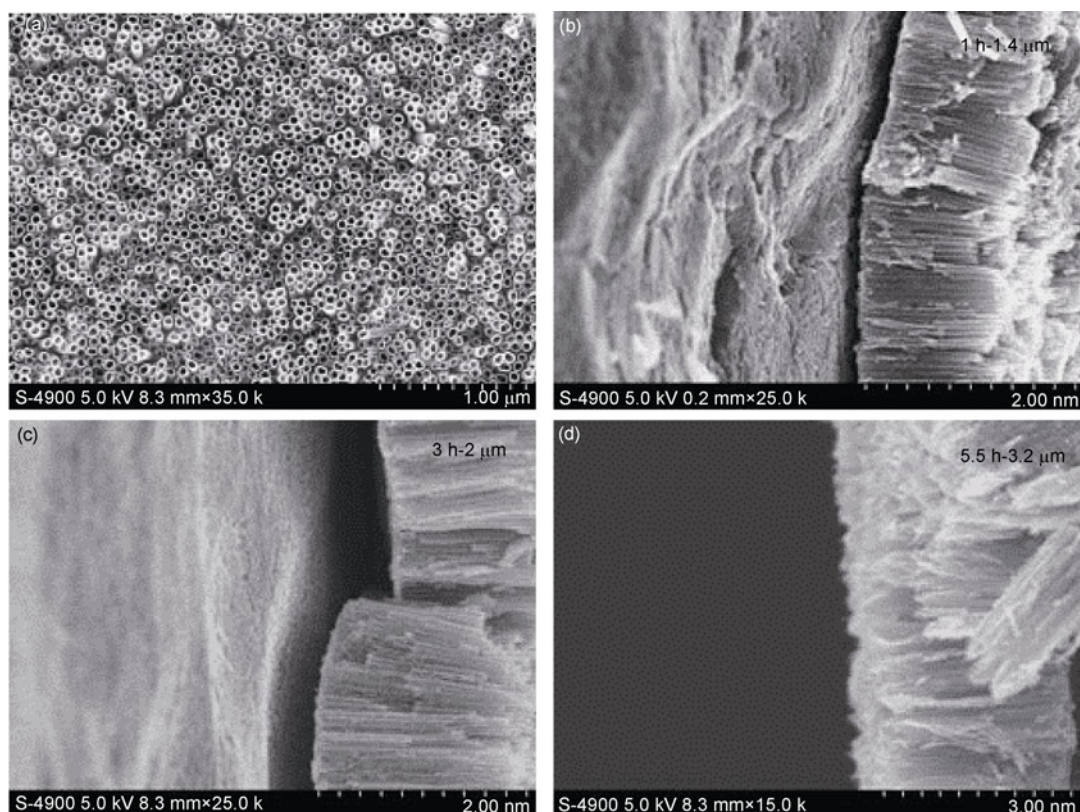


**Figure 6** FE-SEM images of cross-sectional view of the different length nanotubes.

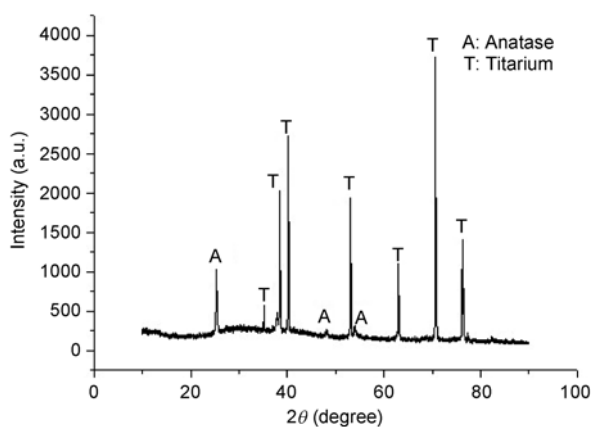


**Figure 7** XRD patterns of TiO<sub>2</sub> nanotubes obtained by anodic oxidation; heat treatment was at 450°C for 1.5 h.

treatment in air at 450°C for 1.5 h, the nanotube arrays crystallize mainly into an anatase phase.

- 1 Wang D A, Liu L F. Continuous fabrication of free-standing TiO<sub>2</sub> nanotube array membranes with controllable morphology for depositing interdigitated heterojunctions. *Chem Mater*, 2010, 22: 6656–6664
- 2 Wang J, Lin Z Q. Dye-sensitized TiO<sub>2</sub> nanotube solar cells with markedly enhanced performance via rational surface engineering. *Chem Mater*, 2010, 22: 579–584
- 3 Gopal K M, Karthik S, Maggie P, et al. Use of highly-ordered TiO<sub>2</sub> nanotube arrays in dye-sensitized solar cells. *Nano Lett*, 2006, 2: 215–218
- 4 Li J Y, Lu N, Quan X, et al. Facile method for fabricating boron-doped TiO<sub>2</sub> nanotube array with enhanced photoelectrocatalytic

- properties. *J Am Chem Soc*, 2008, 47: 3804–3808
- 5 Mohapatra S K, Misra M, Mahajan V K, et al. Synthesis of Y-branched TiO<sub>2</sub> nanotubes. *Mater Lett*, 2008, 62: 1772–1774
- 6 Yuan X L, Zheng M J, Ma L, et al. High-speed growth of TiO<sub>2</sub> nanotube arrays with gradient pore diameter and ultrathin tube wall under high-field anodization. *Nanotechnology*, 2010, 21(40): 405302
- 7 Portan D, Papaefthymiou K, Pirvu C, et al. Manufacturing and characterization of TiO<sub>2</sub> nanotubes on pure titanium surfaces for advanced biomedical applications. *U. P. B. Sci Bull Ser B*, 2011, 73: 181–196
- 8 Marco S, Niranjana P, Roberto C. Use of ionic liquid in fabrication, characterization, and processing of anodic porous alumina. *Nanoscale Res Lett*, 2009, 4: 865–872
- 9 Sanju R, Somnath C R, Maggie P, et al. Synthesis and applications of electrochemically self-assembled titania nanotube arrays. *Phys Chem Chem Phys*, 2010, 12: 2780–2800
- 10 Yeonmi S, Seonghoon L. Self-organized regular arrays of anodic TiO<sub>2</sub> nanotubes. *Nano Lett*, 2008, 8: 3171–3173
- 11 Chen S S, Ling Z Y, Hu X, et al. Controlled growth of branched channels by a factor of  $1/\sqrt{n}$  anodizing voltage? *J Mater Chem*, 2009, 19: 5717–5719
- 12 Mor G K, Shankar K, Paulose M, et al. Enhanced photocleavage of water using titania nanotube arrays. *Nano Lett*, 2005, 5(1): 191–195
- 13 Lin C J, Yu Y H, Chen S Y, et al. Anodic growth of highly ordered titanium oxide nanotube arrays: Effects of critical anodization factors on their photocatalytic activity. *World Acad Sci Eng Technol*, 2010, 65: 1094–1099
- 14 Park H, Kim H G. Characterizations of highly ordered TiO<sub>2</sub> nanotube arrays obtained by anodic oxidation. *Trans Electr Electron Mater*, 2010, 3: 112–115
- 15 Paulose M, Prakasham H E, Varghese O K, et al. TiO<sub>2</sub> nanotube arrays of 1000 μm length by anodization of titanium foil: Phenol red diffusion. *J Phys Chem C*, 2007, 111: 14992–14997
- 16 Liu Z Y, Zhang X T, Nishimoto S, et al. Efficient photocatalytic degradation of gaseous acetaldehyde by highly ordered TiO<sub>2</sub> nanotube arrays. *Environ Sci Technol*, 2008, 42(22): 8547–8551